Study of a compact external magnetic field radial split-cavity oscillator

ZHANG Yun-Jian(张运俭)   MA Qiao-Sheng(马乔生)   LUO Xiong(罗雄)

Institute of Applied Electronics, China Academy of Engineering Physics, Mianyang 621900, China

Abstract: With the experiment result analyses of a coaxial virtual cathode oscillator (CVCO), a new kind of compact radial split cavity oscillator (RSCO) is presented in this paper. On the oscillator, a low resistance tube is formed by using the diode structure of a CVCO, and a radial split-cavity structure is formed by several meshes that cause the electronic beam to transmit. Calculating all kinds of parameter, at the input parameter 350 kV, 27 kA, the numerical simulation results show that the average output microwave power is about 4.0 GW, the microwave frequency is 1.37 GHz, and the electronic efficiency is 42.3%.

Key words: RSCO, high power microwave, CVCO

PACS: 52.65.Rr, 52.59.Ye   **DOI:** 10.1088/1674-1137/35/4/011

1 Introduction

The tendency to develop a high power microwave (HPM) source without an external-magnetic field system is high power and efficiency. In 1992, Barry M. Marder put out the axial split cavity oscillator (ASCO) depending on transit-time effect [1]. In this kind of tube, the electronic beam could be modulated in a short range without an external-magnetic field, but the current density should not be very intensive to avoid the formation of a virtual cathode in the tube, so it's a high impedance microwave tube, and this characteristic affects the output microwave power. In this paper, using the structure of a coaxial virtual cathode, the emission way of electronic beam is changed from the axial to the radial direction, a new kind of HPM source – radial split cavity oscillator (RSCO) – is to be put out. The cavity is radially divided into three resonant cavities by metal meshes. With the beam emitted radially, more powerful current can be transmitted because of the electronic beam density reduced. For the same reason, the space limit current is increased, so a virtual cathode is not easily formed. This feature is the main reason why the output power from an RSCO is more efficient and powerful than that from an ASCO.

2 The structure of the RSCO

With the consideration of the experiment manipuility, the structure characteristic of the coaxial virtual cathode oscillator [2–4] is used. In the structure as shown in Fig. 1, the electronic beam is emitted inward, and the metal meshes are connected to the anode with the mesh shoe region where the upper part of the sustaining region is used as a pouch structure to prevent fire fighting between the anode and cathode. The structure of the RSCO is two annular metal meshes that radially split the coaxial cavity into three cavities, and the electromagnetic field in the cavities is joined through edge coupling effect. The space length between the two meshes is 1.9 cm, and the mesh thickness is 0.1 cm. The mesh, coupling plate and mesh shoe region compose the resonant cavity, and the third cavity is joined in the microwave extraction area. The radial space gap of the third cavity is larger than the other two cavities to enhance the interaction between the electronic beam and the microwave.

The electron collecting area is composed of a mesh and electron absorbed load, whose main operation is to prevent the beam from entering the interaction area again. The internal and outer coaxial waveguide is joined by two stand bars in the microwave extraction area.
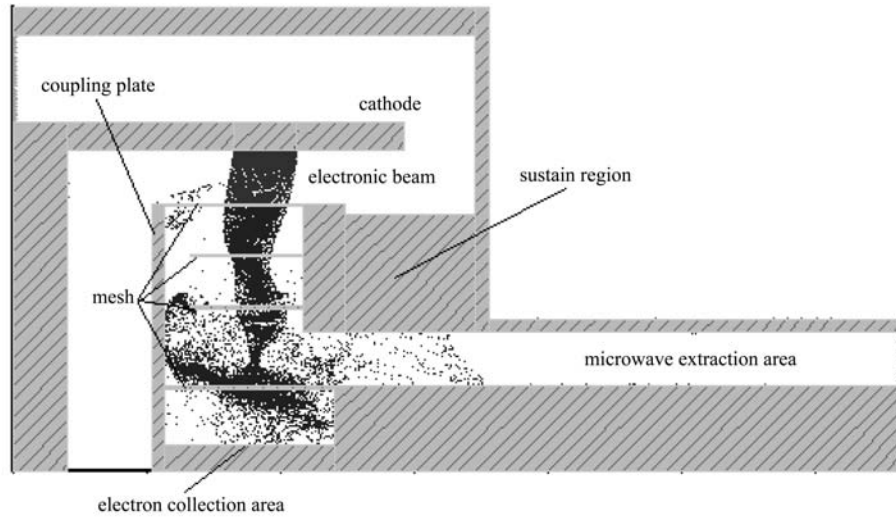
Fig. 1.   Structure of radial split cavity oscillator.

3   Azimuthally symmetric transverse magnetic modes analytic expressions [5–7]

The high frequency geometry of the three radially split cavity oscillator is illustrated in Fig. 2. The coaxial resonant cavity inside the radius is H, the outer radius is $H+R$, the space length between the two meshes is g, the mesh thickness is t, the radial period is p ($p = g+t$, $R = 3p$), the axial direction length is L and the gap between the coupling plate and the mesh is a.
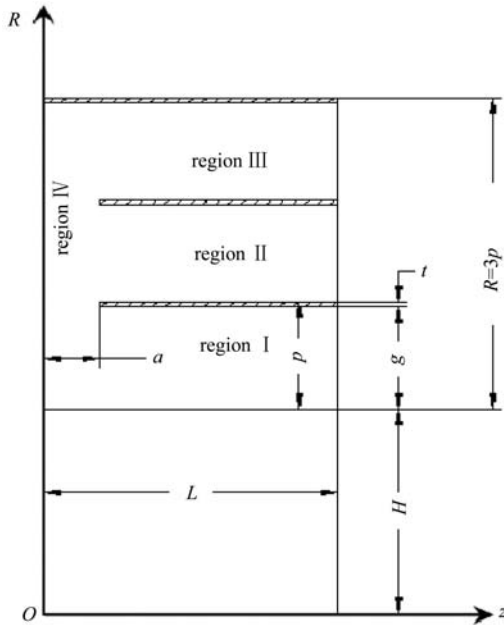

Fig. 2.   High frequency structure of the RSCO.

By using boundary conditions for the Borgnis potential function in conjunction with field matching

conditions at the common interface between the adjacent sub-regions, the analytic expressions of the transverse magnetic (TM) mode axial component of the electricfield (E_z), the radial component of the electricfield field (E_ρ) and the angular component of the magnetic field (H_φ) in various region are given by

$$E_z = \frac{\partial^2 U}{\partial z^2} + k^2 U , \qquad (1)$$

$$E_\rho = \frac{\partial^2 U}{\partial \rho \partial z} , \qquad (2)$$

$$H_\varphi = -j\omega\varepsilon\frac{\partial U}{\partial \rho} , \qquad (3)$$

where $k = \omega/c$ (c is the ray velocity) is the propagation constant, ω is the angular frequency, and ε is the dielectric constant.

For angular symmetry TM modes, U is only the function of the radial component ρ and axial component z. By using the boundary conditions for the Borgnis potential function in conjunction with the field matching conditions at the common interface $z = a$ between adjacent sub-regions, a strict solution of the field in the resonant cavity is obtained. The field matching condition is that arbitrary two components of E_z, E_ρ and H_φ are equivalent at the common interface $z = a$. For simple field expression as Eqs. (1), (2) and (3), the components E_ρ and H_φ are equivalent at $z = a$.

In the region IV ($H \leqslant \rho \leqslant H+R$, $0 \leqslant z \leqslant a$), for the periodic boundary on the radial direction $U_{\rho=H,H+R} = 0$, using Floquet theorem, the field expression is as follows,

$$U(\rho,z) = \sum_{n=-\infty}^{+\infty} A_{4n} \sin[T_n(\rho-H)]f_n(z)\Big/\sqrt{\rho}, \quad (4)$$

where T_n $(n \neq 0)$ is the harmonic component, $k^2 = T_n^2 + \beta_n^2$, T_0 is the fundamental wave, and the field expression is given by

$$E_{\rho 4} = \sum_{n=-\infty}^{+\infty} A_{4n} \frac{T_n \cos[T_n(\rho - H)]}{\sqrt{\rho}} f'_n(z), \qquad (5)$$

$$H_{\varphi 4} = \sum_{n=-\infty}^{+\infty} A_{4n} \frac{T_n \cos[T_n(\rho - H)]}{\sqrt{\rho}} f_n(z), \qquad (6)$$

where

$$f(z) = \begin{cases} \cos(\beta z) & T_n^2 \leqslant k^2 \\ \mathrm{ch}(i\beta z) & T_n^2 \geqslant k^2 \end{cases}. \qquad (7)$$

In the region I $(H \leqslant \rho \leqslant H+g, a \leqslant z \leqslant L)$, using the boundary condition, the field expression is given by

$$E_{\rho 1} = -\frac{A_{10}k}{\rho} \sin[k(z-L)]$$
$$+ \sum_{m=1}^{\infty} A_{1m} T_{1m} \frac{\cos[T_{1m}(\rho - H)]}{\sqrt{\rho}} f'_{1m}(z), \quad (8)$$

$$H_{\varphi 1} = j\omega\varepsilon \frac{A_{10}}{\rho} \cos[k(z-L)]$$
$$- j\omega\varepsilon \sum_{m=1}^{\infty} A_{1m} T_{dm} \frac{\cos[T_{1m}(\rho - H)]}{\sqrt{\rho}} f_{1m}(z), \quad (9)$$

where

$$T_{1m} = \frac{m\pi}{g},$$

$$f_{1m}(z) = \begin{cases} \cos[\beta_{1m}(z-L)] & k^2 \geqslant T_{1m}^2 \\ \mathrm{ch}(i\beta_{1m}L)\mathrm{ch}(i\beta_{1m}z) - \mathrm{sh}(i\beta_{1m}L)\mathrm{sh}(i\beta_{1m}z), \\ & k^2 < T_{1m}^2 \end{cases}$$

$$\beta_{1m}^2 = k^2 - T_{1m}^2, \quad m = 0, 1, 2, 3, \cdots.$$

Like region I, the field expression in region II and III is found to be

$$E_{\rho 2} = -\frac{A_{20}k}{\rho} \sin[k(z-L)]$$
$$+ \sum_{m=1}^{\infty} A_{2m} T_{2m} \frac{\cos[T_{2m}(\rho - H - p)]}{\sqrt{\rho}} f'_{2m}(z), \qquad (10)$$

$$H_{\varphi 2} = j\omega\varepsilon \frac{A_{20}}{\rho} \cos[k(z-L)]$$
$$- j\omega\varepsilon \sum_{m=1}^{\infty} A_{2m} T_{2m} \frac{\cos[T_{2m}(\rho - H - p)]}{\sqrt{\rho}} f_{2m}(z), \qquad (11)$$

$$E_{\rho 3} = -\frac{A_{30}k}{\rho} \sin[k(z-L)]$$
$$+ \sum_{m=1}^{\infty} A_{3m} T_{3m} \frac{\cos[T_{3m}(\rho - H - 2p)]}{\sqrt{\rho}} f'_{3m}(z), \qquad (12)$$

$$H_{\varphi 3} = j\omega\varepsilon \frac{A_{30}}{\rho} \cos[k(z-L)]$$
$$- j\omega\varepsilon \sum_{m=1}^{\infty} A_{3m} T_{3m} \frac{\cos[T_{3m}(\rho - H - 2p)]}{\sqrt{\rho}} f_{3m}(z). \qquad (13)$$

For the physical dimension $H = 4.1$ cm, $p = 2.0$ cm, $g = 1.9$ cm, $R = 6.0$ cm, $L = 6.0$ cm and $a = 1.0$ cm of radially split cavity oscillator, using numerical calculation, the resonant frequency of TM_{020} mode [6] is 1.357 GHz. For the accuracy of the theoretical calculation, the mode in the resonant cavity is solved using 3D electromagnetic calculation soft. The frequency of TM_{020} mode is 1.355 GHz, as shown in Fig. 3, and the result is in agreement with the theoretical calculation.
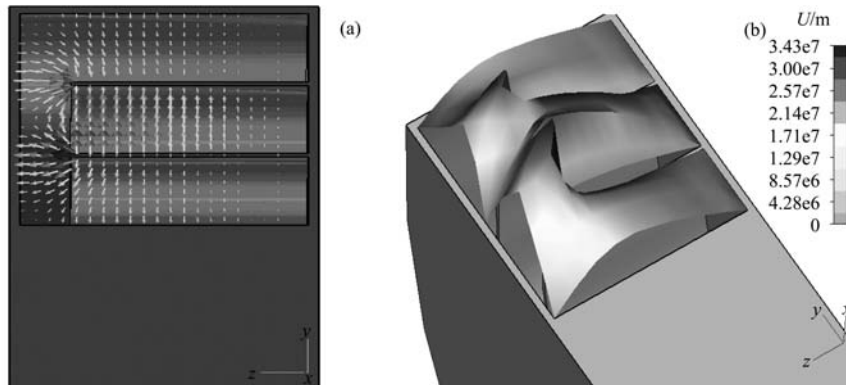

Fig. 3. TM_{020} mode electric field distribution in high frequency structure (a) electric field vector distribution in y-z plane, (b) electric field distribution in three dimensions.

4 Numerical simulation

In the actual numerical simulation, for the output efficiency of HPM, the radial dimension is added to decelerate the velocity of the electron when enhancing the interaction between the electron and the microwave. Fig. 4 is the electric field vector distribution with an electron beam. With Fig. 4, in region i, the electron beam is bunched and decelerated as the microwave power is amplified.
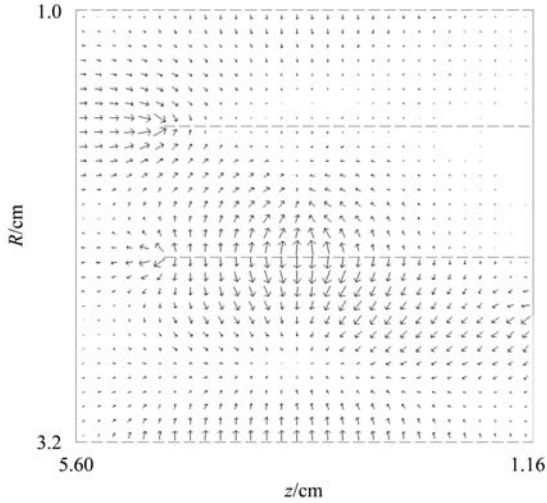

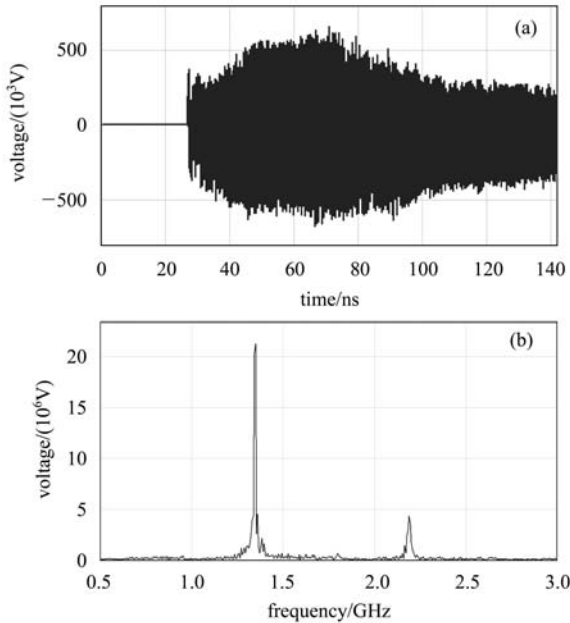Fig. 4. The electric field vector distribution with an electron beam.

Fig. 5. Waveform between the voltage and time (a), and fast fourier transform (b).

The input voltage is 350 kV, and the rising edge is 60 ns; the numerical simulation diode current is 27 kA, and the resistance is about 13.5 Ω. The detailed simulation results are shown in Fig. 5 and Fig. 6.
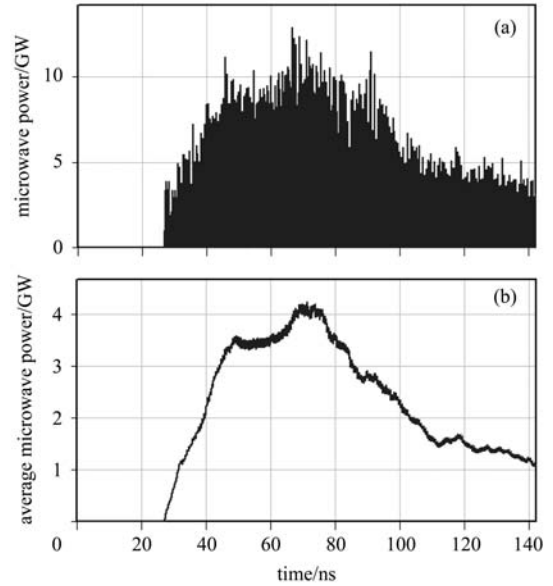

Fig. 6. Waveform between power and time (a), and average power (b).

In Fig. 5(a), the waveform is the relation between time and radiation microwave field voltage, and Fig. 5(b) is the spectrum transformed from Fig. 5(a), the frequency is 1.37 GHz. In Fig. 6(a), the waveform is the relation between time and microwave power, and the maximum average power is about 4.0 GW, as seen in Fig. 6(b), the electronic beam transfer efficiency is about 42.3%. To enhance the interaction between the electric beam and wave, the radial periodic p in region i is larger than the other one to enhance the interaction range, and there is an electron collection area to prevent the electricity from entering the interaction area in the negative direction, so the structure design has increasingly efficient action.

The main elements that affect the output microwave are numerically calculated, and specific calculation results are shown in Tables 1 to 3.

Table 1. The relation between the voltage and the frequency (mesh space 1.9 cm).

voltage/kV	frequency/GHz	average power/GW
100	1.13	0.23
150	1.13	0.5
200	1.21	0.82
250	1.27	2.1
300	1.33	2.9
350	1.37	4.0
400	1.41/1.65	—

Table 2. The relation between the mesh gap
and the frequency (voltage 350 kV).

mesh gap/cm	frequency/GHz
1.1	1.73/1.28
1.3	1.69/1.24
1.5	1.51
1.7	1.37
1.9	1.37
2.1	1.73/1.35
2.3	—

Table 3. The relation between the cavity width
and the frequency (mesh space 1.9 cm).

cavity width/cm	frequency/GHz
5.0	1.70
5.4	1.68
5.8	1.57
6.0	1.37
6.3	1.31
7.0	1.24

In Table 1, with a voltage of 400 kV, a strong virtual cathode is formatted in the mid-cavity, and multi-layer meshes destroy the virtual cathode, so the output HPM is unnstable. Compared with Table 1, the microwave frequency is stable as in the preset resonant cavity, and the voltage has nearly no effect on it, and this is the character of the spilt-cavity oscillator structure. In Table 2, the frequency increases with decreasing gap; and the frequency decreases with increasing cavity width in Table 3. Using the above-mentioned relations, for a given output microwave, the gap and width of the cavity can be adjusted to ensure the compactness of the HPM source. From the data in Table 2 and Table 3, the size and structure of the cavity affect the wave frequency as the conclusion in Table 1.

5 Microwave output

According to the structure feature of the HPM source, the microwave is transmitted using a coaxial waveguide. The radius of the waveguide is 3.2 cm and 5.2 cm, respectively. The output microwave mode is transverse electric and magnetic field (TEM) mode for the RSCO as its structure. The internal and external coaxial waveguides are joined by two stand bars whose fore and-aft traction is about 1/4 of the transmitted wavelength to reduce the reflection of the microwave when inserting the stand bars. For the transverse electric (TE_{11}) mode transforming from TEM mode, one side of the bar near the antenna is filled with dielectric whose length is defined by the equation $L = \pi(\beta_1 - \beta_2)$, where β_1 and β_2 are the TE_{11} mode propagation constant between the dielectric and vacuum [8–10]. To reduce the microwave reflection, the internal waveguide is inserted into the antenna, and this kind of design can reduce the axial size of the HPM source.

The diameter of antenna caliber is 300 mm. After optimum design, the TE_{11} mode main lobe magnitude is 12.4 dB when using mode transform.
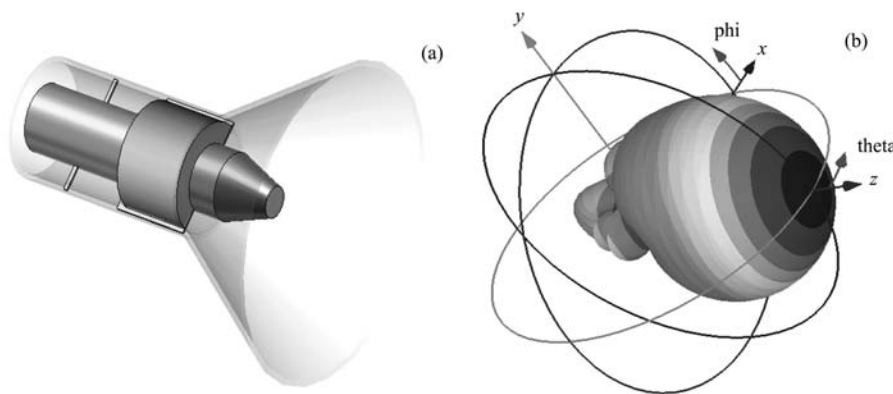

Fig. 7. The antenna with the mode transform structure (a), and the directional diagram of TE_{11} mode (b).

The equation describing the microwave breakdown in the vacuum waveguide is given by

$$f = 1.643 \cdot E^2 e^{-8.5/E} \qquad (14)$$

where f is the microwave frequency (MHz) and E is the electric-field density (MV/m). The breakdown is 330 kV/cm at 1.37 GHz using Eq. (14). From the numerical simulation results in Fig. 5(a), the electric field density is less than 340 kV/cm. The equation describing the single mode power capacity in the coaxial

waveguide is given by

$$P = \frac{1}{120} a^2 E^2 \ln\left(\frac{b}{a}\right). \tag{15}$$

Here, $b = 5.2$ cm is the outer radius, $a = 3.2$ cm is the inside radius and E is the maximum electric field density in the coaxial waveguide. The power capacity is 4.5 GW in the waveguide using $E = 330$ kV/cm, so the HPM in Fig. 6(b) can be transmitted.

6   Summary

Using the structure characteristic of a coaxial virtual cathode oscillator, the electronic beam emitted inward, these ensure the compactness of the structure. With a mode converter, the microwave can be easily extracted. The frequency of the output microwave is mainly related to the resonant cavity structure through numerical simulation. For a given frequency, it can be carried out through the adjustment of the axial and radial size of the cavity. With the analysis for high frequency characteristics, an angular uniform TM mode exists only in the cavity. There is a wider interaction region in the second and third cavity with the analysis for a radial component of the electric field, and this is the main reason for the high efficiency of the output microwave.

References

1   Marer Barry M et al. IEEE Transactions on Plasma Science, 1992, **20**(3): 312

2   LUO Xiong, LIAO Cheng, MENG Fan-Bao et al. High Power Laser and Particle Beams, 2006, **18**: 249 (in Chinese)

3   LUO Xiong, LIAO Cheng, MENG Fan-Bao et al. Acta Phys. Sin., 2006, **55**: 5774 (in Chinese)

4   SHAO Hao, LIU Guo-Zhi. Acta Phys. Sin., 2001, **50**: 2387 (in Chinese)

5   Raymond W. J. Appl. Phys., 1992, **72**(9): 4422

6   FAN Zhi-Kai, LIU Qing-Xiang. Acta Electronica Sinica, 2001, **29**(4): 538

7   ZHANG Ke-Qian, LI D J. Electromagnetic Theory for Microwaves and Optoelectronics. Beijing: Publishing House of Electronics Industry, 2001 (in Chinese)

8   Raymond W. J. Appl. Phys., 1992, **72**(9): 4422

9   Charles M K, Louis F L. IEEE Trans. on AP, 1994, **42**(8): 1188

10   Courtney C C. Electronic Letters, 2002, **38**(11): 496